ELSEVIER

Polymer 41 (2000) 6563–6571

polymer

Miscibility of carboxyl-containing polysiloxane/poly(vinylpyridine) blends

Xu Li[a], S.H. Goh[a,*], Y.H. Lai[a], A.T.S. Wee[b]

[a]*Department of Chemistry, National University of Singapore, 3 Science Drive 3, Singapore, Singapore 117543*
[b]*Department of Physics, National University of Singapore, 3 Science Drive 3, Singapore, Singapore 117543*

Received 14 June 1999; received in revised form 24 September 1999; accepted 25 November 1999

Abstract

Poly(3-carboxypropylmethylsiloxane) (PSI100) and poly(3-carboxypropylmethylsiloxane-*co*-dimethylsiloxane) (PSI*X*, $X = 76, 60, 41, 23$ or 9, denoting the mole percentage of 3-carboxypropylmethylsiloxane unit in the copolymer) were synthesized and characterized. PSI9 is immiscible with both poly(4-vinylpyridine) (P4VPy) and poly(2-vinylpyridine) (P2VPy). The other PSI*X* samples are miscible with both P4VPy and P2VPy over the entire composition range. The shape of glass transition temperature (T_g)-composition curve of the miscible blend system changes from concave to S-shaped and to convex with increasing carboxylic acid content of the copolymer. The T_gs of PSI100/P4VPy and PSI100/P2VPy blends are higher than those calculated from the additivity rule. The miscible PSI23/P4VPy and PSI23/P2VPy blends underwent phase separation upon heating, showing a lower critical solution temperature behavior. The other miscible blends degraded before phase separation could be induced by heating. The specific interactions between P4VPy or P2VPy and PSI*X* were studied by Fourier transform infrared spectroscopy and X-ray photoelectron spectroscopy. The carboxylic acid groups of PSI*X* interact with the pyridine nitrogens through hydrogen-bonding interactions.

Keywords: Miscibility; Carboxyl-containing polysiloxane; Poly(vinylpyridine)

1. Introduction

It has been well established that the formation of a miscible blend requires the presence of favorable interaction between the component polymers. Two dissimilar polymers possessing complementary functional groups are likely to form miscible blends. For example, silanol-containing polymers are miscible with proton-accepting polymers such as poly(*n*-butyl methacrylate) (P*n*BMA) and poly(*N*-vinyl-2-pyrrolidone) through hydrogen-bonding interactions [1–4].

Polysiloxanes such as poly(dimethylsiloxane) (PDMS) are noted for their good thermal stability, low-temperature flexibility, good electrical insulation property, low moisture absorption, biocompatibility and low surface energy [5–11]. However, PDMS is practically immiscible with other polymers because of its lack of interacting groups. To render PDMS some miscibility with other polymers, it is necessary to modify its structure. PDMS containing a small amount of vinyl groups is miscible with poly(ethylene-*co*-methyl acrylate) [12]. Fourier-transform infrared spectroscopy (FT-IR) showed that chemical reaction took place between the two polymers through the vinyl groups of modified PDMS. Chu et al. [13] reported that when one of the methyl groups in the repeating unit of PDMS was changed to 4-hydroxy-4,4′-bis(trifluoromethyl)-butyl group, the resulting polysiloxane became miscible with poly(ethylene oxide) and P*n*BMA.

In this paper, we report the miscibility of poly(3-carboxypropylmethylsiloxane) (PSI100) and poly(3-carboxypropylmethylsiloxane-*co*-dimethylsiloxane) (PSI*X*, $X = 76$, 60, 41, 23 or 9, denoting the mole percentage of 3-carboxypropylmethylsiloxane unit in the copolymer) with poly(2-vinylpyridine) (P2VPy) and poly(4-vinylpyridine) (P4VPy). The miscibility of the blends was ascertained by differential scanning calorimetry (DSC), and the specific interactions in various miscible blends were examined by FT-IR and X-ray photoelectron spectroscopy (XPS).

2. Experimental

2.1. Materials

(3-Cyanopropyl)methyldichlorosilane and dichlorodimethylsilane were supplied by Fluka Chemika-Biochemika Company. P2VPy with a weight-average molecular weight

* Corresponding author. Tel.: +65-874-2844; fax: +65-779-1691.
E-mail address: chmgohsh@nus.edu.sg (S.H. Goh).

0032-3861/00/$ - see front matter
PII: S0032-3861(99)00896-4

Table 1
Characteristics of polymers

	PSI9	PSI23	PSI41	PSI60	PSI76	PSI100
T_g (°C)	−104	−85	−55	−41	−29	−9
M_n (kg mol^{-1})	25	26	30	23	14	6.6
M_w/M_n	2.3	2.2	2.2	2.2	2.0	1.6

(M_w) of 200 kg mol^{-1} was purchased from Polysciences, Inc. P4VPy ($M_w = 200$ kg mol^{-1}) was purchased from Scientific Polymer Products, Inc. PDMS with a viscosity of 60,000 cSt was purchased from Aldrich Chemical Company, Inc. The glass transition temperatures (T_gs) of PDMS, P4VPy, and P2VPy are −125, 153 and 102°C, respectively. All chemicals were used without further purification.

2.2. Synthesis of polymers

(3-Cyanopropyl)methyldichlorosilane (89 g, 0.5 mmol) dissolved in 140 ml of diethylether was dropped into 140 ml of water at 0–5°C over 1 h under vigorous stirring. After extraction with diethylether, the extract was evaporated. To 10 ml residue, 10 ml of water and 10 ml of conc. H_2SO_4 were added. The mixture was stirred at 100°C for 24 h. The aqueous layer was separated and the residue was poured into 2 l of water to obtain a white sticky precipitate. The product was rinsed with water until there was no precipitate formed when the supernatant liquid was added to an aqueous solution of $CaCl_2$. The polymer (PSI100) was then dried in a vacuum oven at 80°C for 2 days. IR, ν (cm^{-1}) 3300–2500 (m, O–H), 1713 (s, C=O), 1000–1100 (s, Si–O); ^{1}H NMR (DMSO-d_6), (ppm), 0.0 (Si–CH_3), 0.5 (Si–CH_2–), 1.5 (C–CH_2–C), 2.2 (–CH_2–COO). PSI100 shows an initial decomposition temperature at 210°C, as shown by thermogravimetry.

PSI*X* samples with different carboxylic acid contents were synthesized according to the above-mentioned method using different feed ratios of (3-cyanopropyl)methyldichlorosilane to dichlorodimethylsilane. In the following discussion, the number after PSI denotes the mole percentage of carboxypropyl group of the copolymer. The carboxypropyl content of the copolymer was determined by NMR according to the following equation:

$$\text{Carboxypropyl content} = 6/(2n + 3)$$

where n is the area ratio of the Si–CH_3 peak to the Si–C–CH_2–C peak. The characteristics of various polymers are summarized in Table 1.

2.3. Preparation of blends

P4VPy, P2VPy and PSI*X* ($X = 100$, 76, 60, 41, 23 or 9) were separately dissolved in ethanol/water (1:1) at a concentration of 10 g l^{-1}. PSI*X*/P4VPy and PSI*X*/P2VPy blends of varying compositions were obtained by mixing appropriate amounts of ethanol/water (1:1) solutions of the polymers.

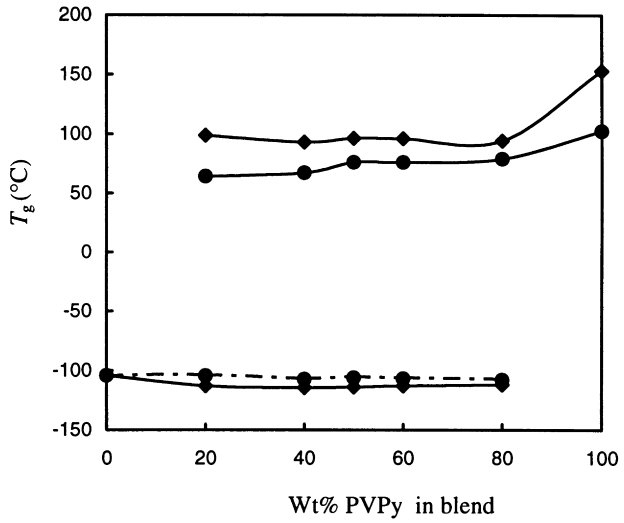

Fig. 1. T_g-composition curve of PSI9/PVPy blends. PSI9/P4VPy blends (◆); PSI9/P2VPy blends (●).

Initial removal of the solvent was done on a hot plate at 70°C. The blends were then dried in a vacuum oven at 60°C for 2 weeks. The dried blends were ground to fine powder and stored in a desiccator.

2.4. T_g measurements

The glass transition temperatures (T_gs) of various samples were measured with a TA Instruments 2920 differential scanning calorimeter using a heating rate of 20°C min^{-1}. Each sample was subjected to several heating/cooling cycles to obtain reproducible T_g values. The initial onset of the change slope in the DSC curve is taken to be the T_g.

2.5. LCST behavior

All the miscible blends were examined for the existence of lower critical solution temperature (LCST) behavior. A film was sandwiched between two microscope coverglasses and heated in a Fisher–Johns melting-point apparatus at a heating rate of about 10°C min^{-1}. The optical appearance of the film was observed with a magnifying glass attached to the apparatus. A transparent film that turns cloudy upon heating indicates the existence of a LCST behavior.

2.6. FT-IR characterization

FT-IR spectra were recorded on a Bio-Rad 165 FT-IR spectrophotometer; 64 scans were signal-averaged with a resolution of 2 cm^{-1}. Samples were prepared by dispersing the blends in KBr and compressing the mixtures to form disks. Spectra were recorded at 130°C to exclude moisture, using a SPECAC high-temperature cell equipped with an automatic temperature controller, which was mounted in the spectrophotometer.

2.7. NMR measurements

Nuclear magnetic resonance (NMR) spectra were recorded on a Bruker ACF 300 spectrometer at 25°C with DMSO-d_6 as the solvent.

2.8. GPC measurements

Average molecular weights and polydispersities of polymers were determined by gel permeation chromatography with a Waters system consisting of a 600E pump, an external column oven of LC-100 set at 25°C and a Waters 410 differential refractometer. The whole system was operated at a flow rate of 0.8 ml min^{-1} using THF as the solvent. A calibration curve was constructed with polystyrene standards.

2.9. XPS measurements

XPS measurements were carried out on a VG Scientific ESCALAB spectrometer using a MgKα X-ray source (1253.6 eV photons). Various blends were ground to fine powders and then mounted on a standard sample stud by means of a double-sided adhesive tape. The X-ray source was run at 12 kV and 10 mA. To compensate for surface charge effects, all core-level spectra were referenced to the C1s neutral carbon peak at a binding energy (BE) of 285.0 eV. The pressure in the analysis chamber was maintained at 10^{-8} mbar or lower during measurements. All spectra were obtained at a take-off-angle of 75° and curve-fitted with VGX-900I software. In spectral deconvolution, the widths (fwhm) of Gaussian peaks were maintained constant for all components in a particular spectrum.

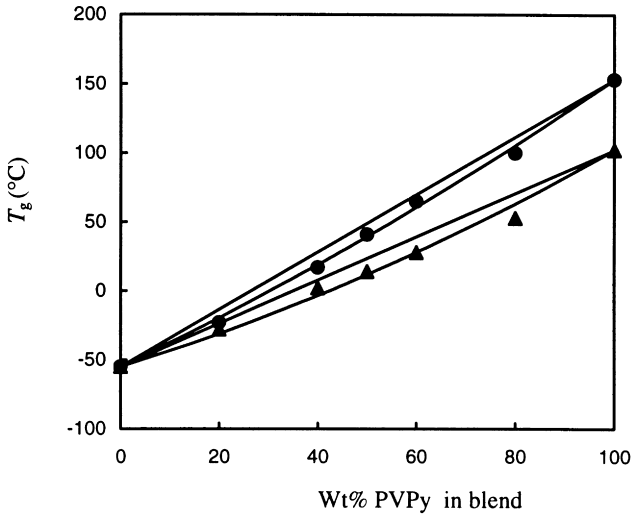

Fig. 3. T_g-composition curve of PSI41/PVPy blends. PSI41/P4VPy blends (●) ($k = 1, q = -33$); PSI41/P2VPy blends (▲) ($k = 1, q = -42$).

3. Results and discussion

3.1. Miscibility of blends

PDMS is immiscible with both P2VPy and P4VPy. The blends were opaque and each blend showed the existence of two T_gs corresponding to those of the component polymers.

PSI9 is also immiscible with P2VPy and P4VPy. The T_g-composition curves of the two blend systems are shown in Fig. 1. The lower T_g values of the blends are close to that of PSI9, indicating that this phase is essentially pure PSI9. However, the upper T_g values are substantially lower than that of P4VPy or P2VPy, indicating the presence of PSI9 in the P4VPy- or P2VPy-rich phase.

However, PSI23 is miscible with both P2VPy and P4VPy. The blends were transparent and each blend showed a single

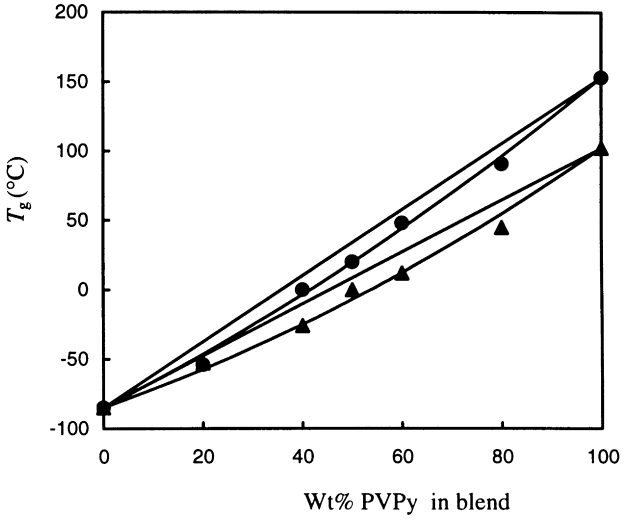

Fig. 2. T_g-composition curve of PSI23/PVPy blends. PSI23/P4VPy blends (●) ($k = 1, q = -52$); PSI23/P2VPy blends (▲) ($k = 1, q = -57$).

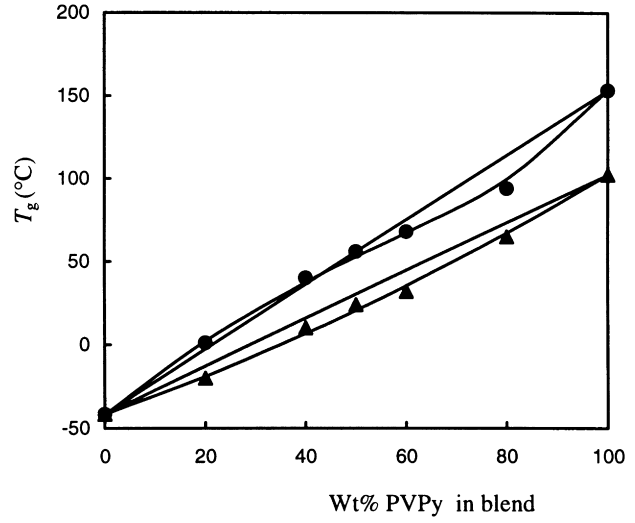

Fig. 4. T_g-composition curve of PSI60/PVPy blends. PSI60/P4VPy blends (●) ($k = 3.3, q = 53$); PSI60/P2VPy blends (▲) ($k = 1, q = -34$).

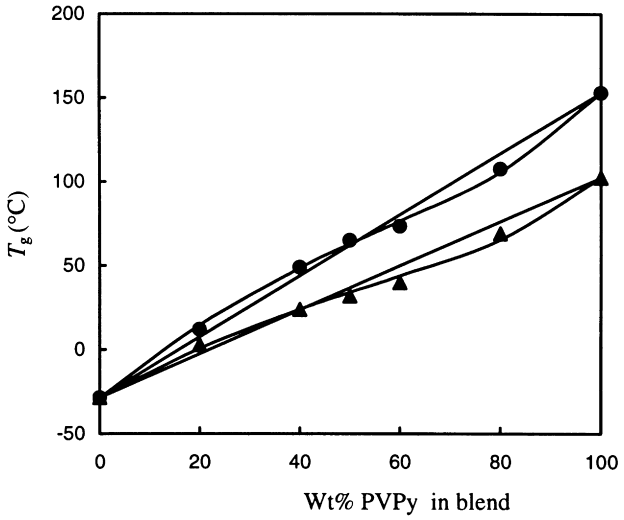

Fig. 5. T_g-composition curve of PSI76/PVPy blends. PSI76/P4VPy blends (●) ($k = 2.9, q = 95$); PSI76/P2VPy blends (▲) ($k = 3, q = 61$).

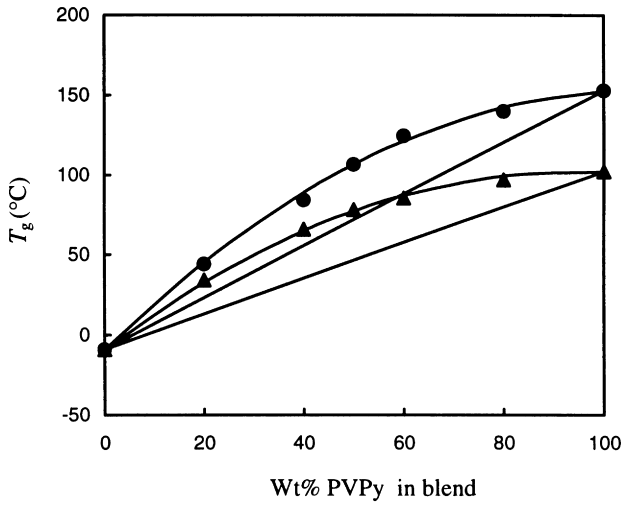

Fig. 6. T_g-composition curve of PSI100/PVPy blends. PSI100/P4VPy blends (●) ($k = 1, q = 138$); PSI100/P2VPy blends (▲) ($k = 1, q = 123$).

T_g. The T_g-composition curves are shown in Fig. 2. The T_g values are lower than those calculated from the linear additivity rule. Therefore, the presence of 23 mol% carboxypropyl group in PSI*X* is sufficient to achieve miscibility with poly(vinylpyridine)s

Similarly, PSI41, PSI60, PSI76 and PSI100 are all miscible with P2VPy and with P4VPy as shown by the transparency of the blends and the existence of a single T_g in each blend. The T_g-composition curves of the various miscible blend systems are shown in Figs. 3–6. One interesting point to note is the change in the shapes of these curves with increasing carboxypropyl content in PSI*X*. At a low carboxypropyl content, the T_g values are lower than those calculated by the linear additivity rule and the curve is concave. At a higher carboxypropyl content, the curve becomes S-shaped. For PSI100, the T_g values of the blends are higher than those calculated from the additivity rule, leading to a convex curve. All the T_g-composition curves can be described by the Kwei equation [14,15].

$$T_g(\text{blend}) = [(w_1 T_{g1} + k w_2 T_{g2})/(w_1 + k w_2)] + q w_1 w_2$$

where w_i and T_{gi} are the weight fraction and T_g of polymer i in the blend, respectively, and k and q are fitting constants. All the curves as shown in Figs. 1–6 were drawn using the appropriate k and q values. Kwei [14] pointed out the term $(w_1 T_{g1} + k w_2 T_{g2})/(w_1 + k w_2)$ in the equation is a commonly used expression for the T_g of polymer mixtures which can be derived formally by using the additive rule of the entropy or the volume of the mixture, and the quadratic term $q w_1 w_2$ is proportional to the number of specific interactions in the blends. The mixing term is concave toward the weight-average line where the interaction term is convex toward it. The combination of these two terms may result in the S-shaped curve as shown in Figs. 4 and 5. When the interaction term predominates (larger q value), the T_g-composition curve will then be convex as shown in Fig. 6. The q value increases with increasing carboxypropyl content of PSI*X*, reflecting an increase in the number of interactions. The changes in the shape of T_g-composition curve and the q value with copolymer composition are therefore the result of increasing number of carboxypropyl groups.

The miscible P4VPy/PSI23 and P2VPy/PSI23 blends developed cloudiness upon heating to 170–200°C, showing the existence of LCST behavior. However, all the other miscible blends involving PSI*X* with higher carboxypropyl content degraded before phase separation could be induced by heating. The results could be taken to indicate that as the carboxypropyl content of PSI*X* becomes higher, the interaction between P4VPy or P2VPy and PSI*X* becomes more intense such that degradation of polymers occurs before phase separation could take place.

3.2. FT-IR characterization

Various PSI100/P4VPy and PSI100/P2VPy blends were studied by FT-IR at 130°C, focussing on the hydroxyl stretching region and carbonyl stretching region of PSI100, and the pyridine ring stretching region. The spectra of the component polymers and all the blends in these regions are shown in Figs. 7 and 8.

The IR spectrum of PSI100 shows the characteristics typical of an associated polyacid. The hydroxyl stretching region exhibits a broad band around 3100 cm^{-1} and a satellite band around 2620 cm^{-1}, which can be attributed to dimeric carboxylic acid groups as commonly observed in other carboxylic acids [17–19]. The carbonyl stretching band around 1710 cm^{-1} is broad and comprises two overlapping carbonyl stretching modes of free and self-associated carboxylic acid groups in PSI100. The latter is at a lower wavenumber than the former.

Upon mixing PSI100 with poly(vinylpyridine)s, there are significant changes in the hydroxyl stretching region and

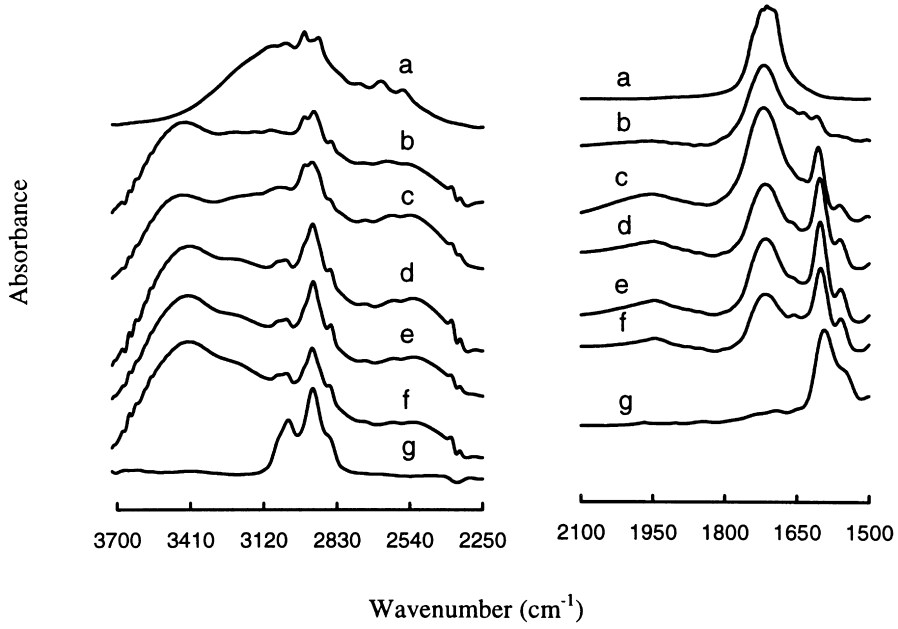

Fig. 7. FT-IR spectra of PSI100/P4VPy blends: (a) 0 wt%; (b) 20 wt%; (c) 40 wt%; (d) 50 wt%; (e) 60 wt%; (f) 80 wt%; and (g) 100 wt% P4VPy.

carbonyl stretching region of PSI100 in the blends. The hydroxyl-stretching region shows an increasing contribution at wavenumbers higher than those corresponding to the dimers. This change is particularly obvious in the PSI100/P4VPy blends than in the PSI100/P2VPy blends. Apparently, the dimeric association of carboxylic acid groups is replaced by interpolymer interactions. There is a remarkable shift of the satellite band (2620 cm^{-1}) towards a lower wavenumber and the intensity increases with increasing poly(vinylpyridine) content in the blends. The other striking feature in Figs. 7 and 8 is the presence of a weak broad band centered around 1930 cm^{-1} which becomes more distinct with increasing poly(vinylpyridine) content in the blends. The development of the 1930 cm^{-1} band was also observed in poly(ethylene-*co*-methacrylic acid)/P2VPy and poly(monomethyl itaconate)/poly(vinylpyridine) blends [18,19]. Blending of PSI100 with P4VPy and P2VPy also brings along changes in the carbonyl region. The original broad carbonyl band becomes sharper and the peak maximum moves to a higher wavenumber. The changes are consistent with the liberation of carbonyl groups from the carboxylic acid dimer when PSI100 interacts with P4VPy and P2VPy.

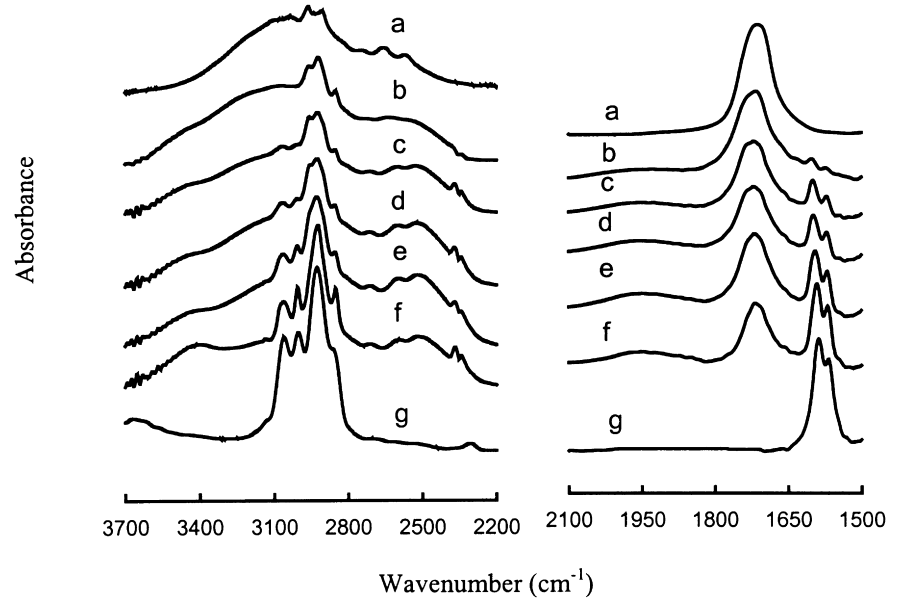

Fig. 8. FT-IR spectra of PSI100/P2VPy blends: (a) 0 wt%; (b) 20 wt%; (c) 40 wt%; (d) 50 wt%; (e) 60 wt%; (f) 80 wt%; and (g) 100 wt% P2VPy.

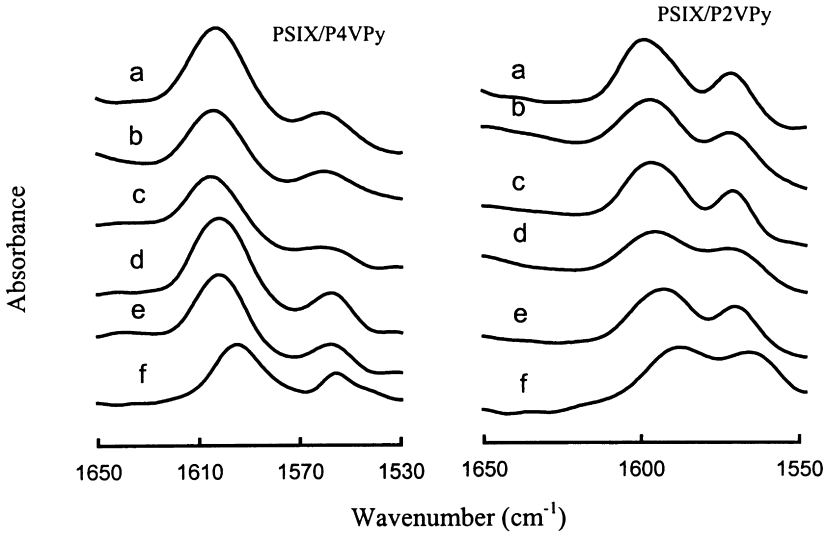

Fig. 9. FT-IR spectra of PSI*X*/PVPy (50:50) blends: (a) PSI100; (b) PSI76; (c) PSI60; (d) PSI41; (e) PSI23; and (f) PVPy.

Similar changes were also observed in poly(monoalkyl itaconate)/poly(vinylpyridine) blends [17,18].

The characteristic pyridine ring modes also show changes upon mixing PSI100 with poly(vinylpyridine)s. As shown in Figs. 7 and 8, P4VPy and P2VPy exhibit a pyridine ring band at 1597 and 1590 cm^{-1}, respectively. However, these bands shift slightly to higher wavenumbers with increasing PSI100 content in the blends. The shift is due to an increase in the rigidity of the pyridine ring arising from interpolymer interaction [18]. The pyridine ring band in P4VPy blends shows a larger shift (9 cm^{-1}) than that in the P2VPy blends (5 cm^{-1}). A similar trend was also observed for poly(monomethyl itaconate)/poly(vinylpyridine) blends [18]. This result may be taken to indicate that P4VPy interacts more strongly with PSI100 than P2VPy does. In cases where the pyridine nitrogen is protonated by a polyacid, the existence of pyridinium ion is shown by the appearance of a new band at 1634 cm^{-1} for P4VPy and 1620 cm^{-1} for P2VPy [16,20,21]. The absence of these bands in various PSI100/P4VPy and PSI100/P2VPy blends shows that the pyridine nitrogens are not protonated. This result indicates that the interaction between PSI100 and P4VPy or P2VPy is a hydrogen-bonding interaction but not an ionic interaction.

Fig. 9 shows the pyridine ring band of various PVPy/PSI*X* (50:50) blends. In both cases, the pyridine ring band at 1597 cm^{-1} for P4VPy and at 1590 cm^{-1} for P2VPy gradually shift toward higher wavenumbers with increasing carboxypropyl content of PSI*X*. Therefore, the results show that increasing carboxypropyl content of PSI*X* leads to an increase in the intensity of hydrogen-bonding interaction.

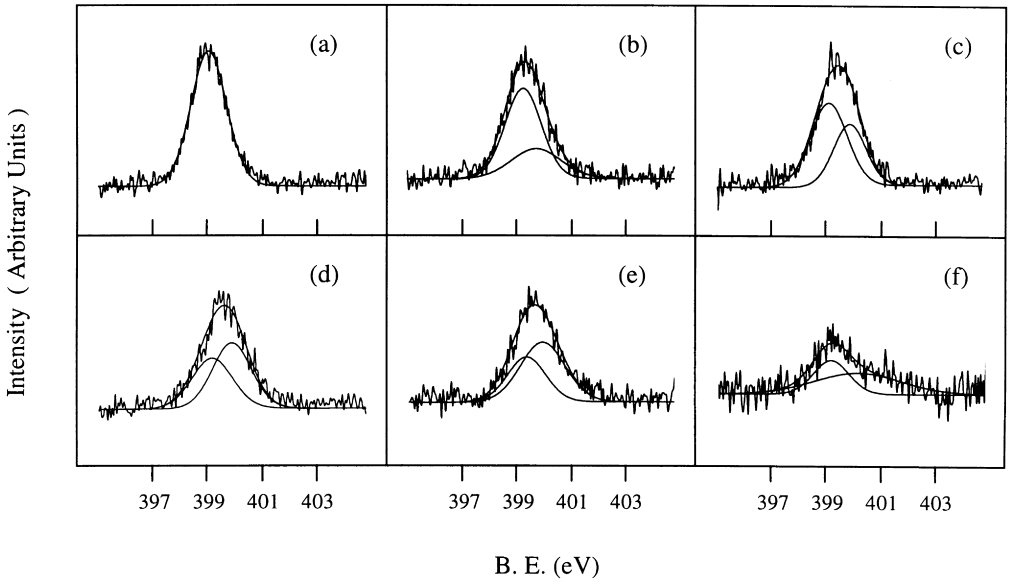

Fig. 10. N1s core-level spectra of P4VPy/PSI100 blends: (a) 100 wt%; (b) 80 wt%; (c) 60 wt%; (d) 50 wt%; (e) 40 wt%; and (f) 20 wt% P4VPy.

Table 2
Characteristics of PSI100/P4Vpy blends

Blend sample number	1	2	3	4	5
Mole fraction of PSI100 in the bulk	0.15	0.32	0.42	0.52	0.74
Mole fraction of PSI100 in the surface region	0.29	0.42	0.58	0.64	0.78
N1s BE (eV)	399.3, 399.8	399.3, 399.8	399.3, 400.0	399.3, 400.1	399.3, 400.2
Fraction of high-BE N1s peak	0.31	0.39	0.55	0.60	0.62

Table 3
Characteristics of PSI100/P2VPy blends

Blend sample number	1	2	3	4	5
Mole fraction of PSI100 in the bulk	0.15	0.32	0.42	0.52	0.74
Mole fraction of PSI100 in the surface region	0.27	0.37	0.48	0.55	0.81
N1s BE (eV)	399.3, 399.7	399.3, 399.8	399.3, 399.9	399.3, 399.9	399.3, 399.9
Fraction of high-BE N1s peak	0.26	0.33	0.49	0.55	0.59

3.3. XPS characterization

We have recently used XPS to study intermolecular interactions in polymer blends and complexes [20–24]. Since the binding energy (BE) of a core-level electron depends on its chemical environment within the molecule, the XPS spectrum provides information on the type and number of different species of a given atom in the molecules. When P4VPy and P2VPy undergo hydrogen-bonding interactions with weak acidic polymers such as poly(*p*-vinylphenol), the BE value of N1s electron is increased by 1 eV or less. On the contrary, when P4VPy and P2VPy are protonated by strong acidic polymers such as poly(styrenesulfonic acid) and poly(vinylphosphonic acid), the BE value of N1s electron is increased by more than 2 eV. Therefore, XPS provides a convenient means to confirm whether P4VPy and P2VPy are involved in hydrogen-bonding or ionic interactions with PSI*X*.

The surface compositions of the blends can be calculated from the Si/N peak area ratios after correction with the appropriate sensitivity factors. As shown in Tables 2 and 3, the mole fraction of PSI100 in the surface region of a blend is higher than that in the bulk. The surface region of a polymer blend is enriched with the polymer with a lower surface energy [25–27]. Since polysiloxanes are noted for

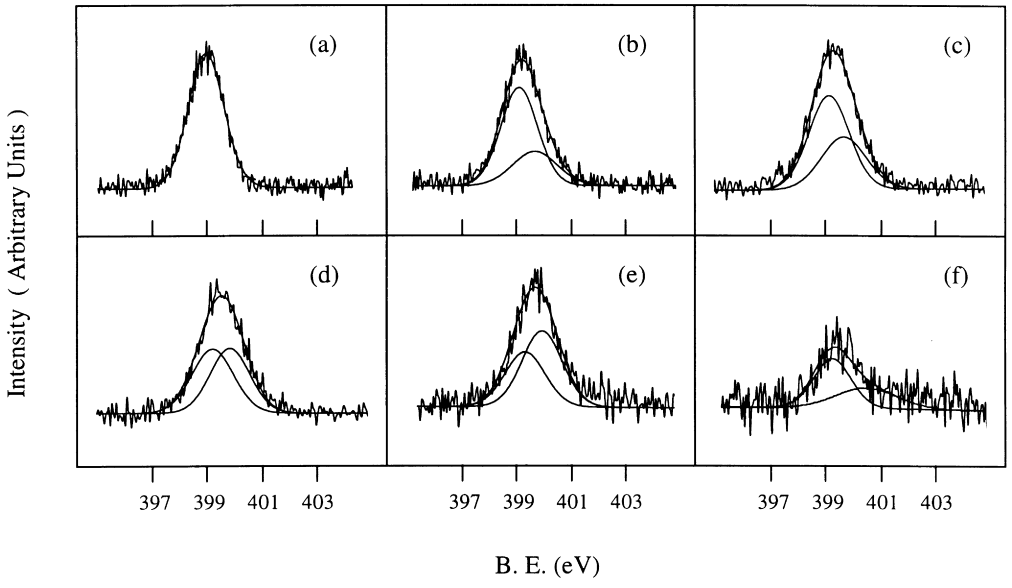

Fig. 11. N1s core-level spectra of P2VPy/PSI100 blends: (a) 100 wt%; (b) 80 wt%; (c) 60 wt%; (d) 50 wt%; (e) 40 wt%; and (f) 20 wt% P2VPy.

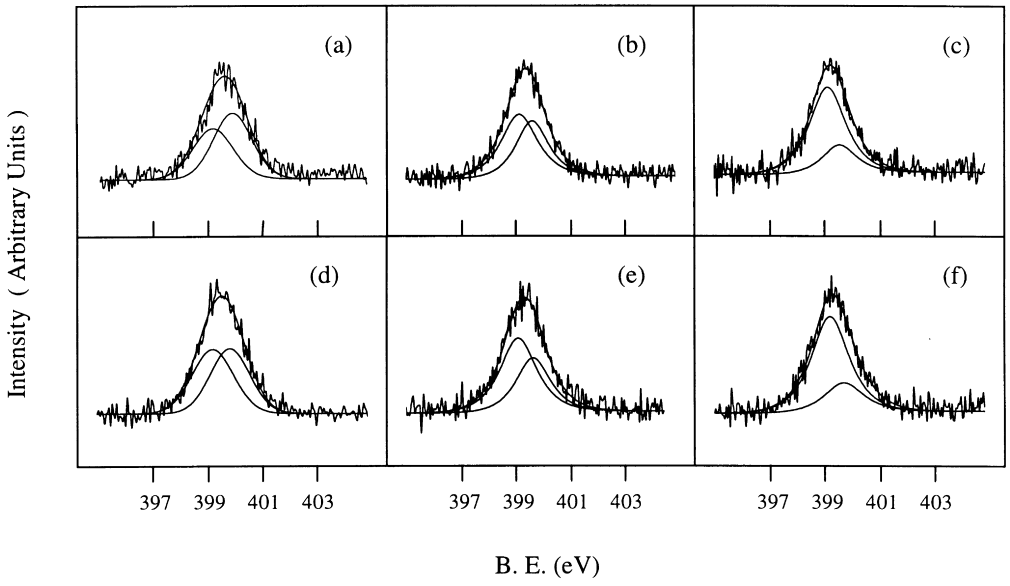

Fig. 12. N1s core-level spectra of PVPy/PSI*X* (50:50) blends: (a) P4VPy/PSI100; (b) P4VPy/PSI76; (c) P4VPy/PSI23; (d) P2VPy/PSI100; (e) P2VPy/PSI76; and (f) P2VPy/PSI23.

their low surface energies, one would expect the surface regions of the PSI100/P4VPy and PSI100/P2VPy blends to be enriched with PSI100, and this is confirmed experimentally.

Fig. 10 shows the N1s core-level spectra of P4VPy and PSI100/P4VPy blends. The N1s spectrum of P4VPy features a symmetric peak at 399.3 eV. However, the N1s peaks of the blends are broader and each peak can be deconvoluted into two component peaks, with one still remaining at 399.3 eV and the other appearing around 400.0 eV. The appearance of the high-BE peak indicates that some of the pyridine nitrogens interact with the carboxyl group of PSI100. Since the BE-shift is about 0.7 eV, the interaction between P4VPy and PSI100 is hydrogen-bonding but not ionic interaction. The conclusion is in accordance with that revealed by FT-IR studies as mentioned earlier. The fraction of interacting P4VPy units can be estimated from the areas of the deconvoluted peaks. As shown in Table 2, the fraction of the N1s high-BE component peak increases with increasing PSI100 content in the blends.

The N1s core-level spectra of P2VPy and PSI100/P2VPy blends are shown in Fig. 11. Similarly, a high-BE N1s peak around 400.0 eV is developed in each blend, showing the existence of hydrogen-bonding interactions. However, the fractions of interacting pyridine units are slightly higher in the PSI100/P4VPy blends than those in the PSI100/P2VPy blends. The results confirm the general view that the nitrogen in P4VPy is more accessible to hydrogen-bonding interaction than that in P2VPy.

Fig. 12 compares the N1s core-level spectra of several PVPy/PSI*X* (50:50) blends. For both P4VPy/PSI*X* and P2VPy/PSI*X* blend systems, increasing carboxypropyl content of the PSI*X* sample leads to an increase in the intensity of the high-BE N1s peak, showing that more pyridine nitrogens are involved in hydrogen-bonding interactions when the PSI*X* sample contains more carboxypropyl groups. Fig. 12 also shows that the high-BE N1s peak of the P4VPy/PSI*X* blend is slightly more intense than the corresponding P2VPy/PSI*X* blend.

4. Conclusions

PDMS is immiscible with P4VPy and P2VPy. However, PSI*X* containing 23 mol% or more carboxylic acid group is miscible with P4VPy and P2VPy. Miscibility arises from hydrogen-bonding interaction between the acid groups of PSI*X* and the pyridine nitrogens. Both FT-IR and XPS show that the hydrogen-bonding interactions between P4VPy or P2VPy and PSI*X* become more intense with increasing carboxypropyl content of PSI*X*. The increase of the intensity of hydrogen-bonding interaction also leads to a change in the shape of the T_g-composition curve.

References

[1] Lu S, Pearce EM, Kwei TK. J Polym Sci, Part A: Polym Chem 1994;32:2607.
[2] Lu S, Pearce EM, Kwei TK. J Macromol Sci, Pure Appl Chem 1994;A31:1535.
[3] Lu S, Pearce EM, Kwei TK. Polym Adv Technol 1996;7:553.
[4] Lu S, Pearce EM, Kwei TK, Chu EY. J Polym Sci, Part A: Polym Chem 1996;34:3163.
[5] Feldman D, Barbalata A. Synthetic polymers. London: Chapman and Hall, 1996.
[6] Deborah DL. Materials for electronic packaging. London: Butterworths–Heinemann, 1995.
[7] He Y, Yang JP, Li HS, Hung PC. Polymer 1998;39:3393.

[8] Stern SA, Shah VM, Hardy BJ. J Polym Sci, Polym Phys 1987;25:1263.
[9] Hill DJT, Killeen MI, O'Donnell JH, Pomery PJ, John DSt. J Appl Polym Sci 1996;61:1757.
[10] Yilgor I, McGrath JE. Adv Polym Sci 1988;86:1.
[11] Anne M, Michael G, John KP, Kenneth JW. Polymer 1999;40:419.
[12] Santra RN, Roy S, Bhowmick AK, Nando GB. Polym Engng Sci 1993;33:1352.
[13] Chu EY, Pearce EM, Kwei TK, Yeh TF, Okamato Y. Makromol Chem, Rapid Commun 1991;12:1.
[14] Kwei TK. J Polym Sci, Polym Lett Ed 1984;22:307.
[15] Pennachia JR, Pearce EM, Kwei TK, Bulkin BJ, Chen JP. Macromolecules 1986;19:973.
[16] Zhou X, Goh SH, Lee SY, Tan KL. Appl Surf Sci 1998;126:141.
[17] Velada JL, Cesteros LC, Meaurio E, Katime I. Polymer 1995; 36:2765.
[18] Cesteros LC, Velada JL, Katime I. Polymer 1995;36:3183.
[19] Lee JY, Painter PC, Coleman MM. Macromolecules 1988;21:954.
[20] Zhou X, Goh SH, Lee SY, Tan KL. Polymer 1998;39:3631.
[21] Zhou X, Goh SH, Lee SY, Tan KL. Polymer 1997;38:5333.
[22] Goh SH, Lee SY, Zhou X. Macromolecules 1998;31:4260.
[23] Goh SH, Lee SY, Dai J, Tan KL. Polymer 1996;37:5305.
[24] Zhou X, Goh SH, Lee SY, Tan KL. Appl Surf Sci 1997;119:60.
[25] Bhatia QS, Pan DH, Kobertein JT. Macromolecules 1988;21:2166.
[26] Schmidt JJ, Gardella Jr. JA, Salvati Jr. L. Macromolecules 1989; 21:4489.
[27] Goh SH, Chan HSO, Tan KL. Appl Surf Sci 1991;52:1.